Author: Calkoen, Emmeline E.
Title: Atrioventricular septal defect : advanced imaging from early development to long-term follow-up
Issue Date: 2016-03-24

Chapter 3.2

Characterization and improved quantification of left ventricular inflow using streamline visualization with 4DFlow MRI in healthy controls and patients after atrioventricular septal defect correction

Emmeline E. Calkoen, Arno A.W. Roest, Lucia J.M. Kroft, Rob J. van der Geest, Monique R.M. Jongbloed, Pieter J. van den Boogaard, Nico A. Blom, Mark G. Hazekamp, Albert de Roos and Jos J.M. Westenberg

J Magn Reson Imaging. 2015;41:1512-20

ABSTRACT

Purpose

To evaluate trans-left atrioventricular valve (LAVV) blood flow and optimize left ventricular inflow quantification in healthy controls and patients after atrioventricular septal defect (AVSD) correction.

Materials and Methods

Twenty-five patients after AVSD correction and 25 controls underwent 4DFlow MRI. Using streamline visualization in four- and two-chamber views, inflow direction at early and late filling was defined at the annulus level and at the peak inflow velocity (PIV) level. Trans-LAVV flow volume and velocity were assessed from a static 2D-multiplanar-reformat (MPR), a 4D-MPR tracking LAVV annulus and a 4D-MPR tracking the PIV-level, angulated perpendicular to the inflow.

Results

In patients, on average 9 more laterally directed inflow was found at the PIV-level compared with controls. In controls, 4DFlow velocity mapping with LAVV annulus tracking resulted in lower absolute error with aortic flow (3 (1–8) mL) than with static 2D-MPR (7 (4–16) mL, P ¼ 0.001). In patients, 4D-MPR tracking the PIVlevel, resulted in lower absolute error with aortic flow (2 (1–4) mL) than with 4D-MPR LAVV annulus tracking (6 (2–10) mL, P = 0.003).

Conclusion

Streamline visualization of 4DFlow MRI data revealed dynamic trans-LAVV inflow and more lateral flow after AVSD correction. Streamline visualization improved trans-LAVV flow quantification as the positioning and angulation of the measurement plane was optimized, allowing an accurate assessment of left ventricular inflow.

INTRODUCTION

Quantification of blood flow over the atrioventricular valve (AVV) is essential in the evaluation of valve function and ventricular filling [1]. Left atrioventricular valve (LAVV) dysfunction and diastolic dysfunction are both indicators of cardiovascular morbidity and mortality [2]. Moreover, disturbances of ventricular inflow have been shown to reduce the effi- ciency of the heart pump [3]. After correction of an atrioventricular septal defect (AVSD), LAVV morphology is changed substantially [4], but limited data are available on the physiological consequences of altered ventricular inflow.

Time-resolved 3D magnetic resonance imaging (MRI) with three-directional velocity-encoding (VE), termed 4DFlow, can be applied to obtain timedependent distribution of blood flow velocities in the cardiac chambers during the whole cardiac cycle. Streamlines are lines representing the blood flow direction at one instant in time, as these lines are tangent to the local velocity vectors, connecting at all points along the direction of these lines [5]. Moreover, they can be presented with color-coding according to velocity magnitude [6] and therefore allow localization of the peak inflow velocities.

Blood flow over the atrioventricular valves can be quantified using a static 2D plane, which is commonly used in a clinical setting, but this approach has been shown to overestimate flow volume as the annulus plane moves through the static measurement plane [7]. With 4D retrospective valve tracking, blood flow over the atrioventricular valves can be quantified more accurately, with the measurement plane adapting to the valve motion, as was validated in phantoms and volunteers [8]. In these reports, valve tracking was used to follow the anatomical annular plane, assuming blood flow to be orthogonal to the annulus during LV filling. Errors in the location and angulation of the reformatting plane may affect flow assessment [9]. Furthermore, changes in inflow direction during the cardiac cycle may also affect the assessment of diastolic parameters derived from AVV flow, measured with echocardiography and MRI [10].

We hypothesize that knowledge of the LV inflow pattern, depicted with streamline visualization in healthy controls and patients after AVSD correction, will aid the retrospective valve tracking procedure: by locating the peak inflow velocity near the tips of the LAVV leaflets and aligning the measurement plane perpendicular to the inflow direction, flow quantification may be improved.

Subsequently, the purpose of our study was to characterize trans-LAVV blood forward flow in healthy controls and patients after AVSD correction using 4DFlow MRI with streamline visualization and to assess the effect of optimal positioning of the measurement plane to assess the LAVV forward flow.

MATERIAL AND METHODS

Study Population

The study was approved by the local Ethics Committee and written informed consent was obtained from all participants or their parents. Between October 2012 and July 2013, 28 patients with a history of corrected AVSD were prospectively and consecutively enrolled in the study from an available surgical database [11]. Patients younger than 8 years, with pacemaker dependency and/or Down syndrome were excluded. Twenty-five controls with a similar age with no history of cardiac disease were included for comparison.

MRI

Whole-heart 4DFlow was obtained using a 3T-MRI scanner (Ingenia, Philips Medical Systems, Best, The Netherlands) with maximal gradient amplitude of 45 mT/m for each axis and a slew rate of 200 T/m/sec. A combination of FlexCoverage Posterior coil in the tabletop with a dStream Torso coil was used, providing up to 32 coil elements for signal reception. In the majority of patients (21 out of 25), gadolinium contrast agent (0.015 mmol/kg body weight, Dotarem, Guerbet, Aulnay-sous-Bois, France) was administrated just before the 4DFlow acquisition. Velocity encoding of 150 cm/s was used in all three directions, spatial resolution 2.3×2.3×3.0–4.2mm, flip angle 10 °, echo time (TE) 3.2 msec, and repetition time (TR) 7.7 msec, resulting in a maximal true temporal resolution of 4 x TR = 31 msec. Parallel imaging was performed using SENSE with factor of 2 and echo planar imaging with factor 5 was used for acquisition acceleration. The commercially available concomitant gradient correction and local phase correction filter were applied. The 4DFlow acquisition time was, for a typical heart rate of 60–80 beats per minute, on average 8–10 minutes. Furthermore, a two-chamber view of the left ventricle, a four-chamber view as well as a short-axis stack of slices, to measure left ventricular volumes and compute the ejection fraction (EF), were acquired with a steady-state free-precession sequence with TE/TR 1.5/3.0; 350mm field of view, 8 mm section thickness; 45 ° flip angle; spatial resolution 1.0×1.0×8.0mm, three signal averages and parallel imaging with SENSE factor 2. Manual contour segmentation of LV volume was performed on the short axis stack to compute EF (EF = LV end diastolic volume – LV end systolic volume / LV end diastolic volume). During all scans, free breathing was allowed and no respiratory compensation was performed, retrospective vectorcardiogram-gating was performed, and for all acquisitions 30 phases were reconstructed representing one average cardiac cycle.

Image Analysis: Characterization of LAVV Forward Flow

Image analysis was performed using in-house developed Mass software. 2D streamlines were generated based on image pixels within the LV cavity exceeding a minimum velocity of 10 cm/s, defined as candidate seed points. Streamlines were computed by applying a simple Euler integration method in both forward and backward directions using a step size of 1 pixel dimension and using bilinear image interpolation. Integration was terminated when either the velocity was below 10 cm/s, or the trace length reached a length of 80 screen pixels. To avoid visual cluttering of the generated streamlines, images were displayed enlarged on the computer monitor and the distance between seed points was forced to be 20 screen pixels at minimum. Three angles were measured in the twoand four-chamber view to characterize the valve morphology and the inflow pattern: the angle between the annulus and long-axis (Fig. 1A, angle 1), the angle between annulus and inflow direction at annulus level (Fig. 1B, angle 2) and the angle between the inflow direction and a plane parallel to the annulus at the level of peak inflow velocity (PIV) (Fig. 1B, angle 3). Angle 1 and angle 2 were measured at E-peak and Apeak, while angle 3 was measured only at E-peak, as the highest inflow velocity appeared at the E-peak. The timepoints of E- and A-peak were defined based on the flow-time curve calculated from velocity mapping after retrospective valve tracking. Finally, to combine the effect of annulus movement and flow direction through the annulus, we calculated the inflow angle defined as

Figure 1. Inflow angles.

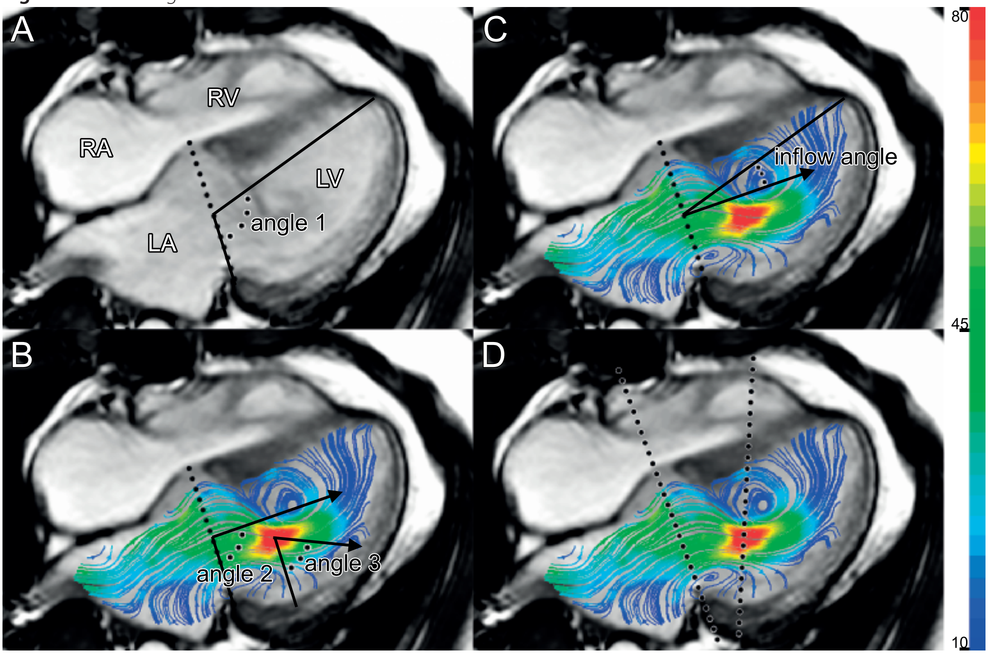

Streamline representation with velocity color coding (in cm/s) of LV inflow pattern illustrates the measured angles in the four-chamber view. A: The angle between annulus and long-axis (angle 1), where the annulus was manually identified as the line between the septal and lateral attachment of the LAVV and the long-axis was recognized as the line through the center of the annulus and the apex. B: The angles between annulus and inflow at the annulus level (angle 2) and peak inflow velocity level (angle 3). C: The inflow angle calculated as the difference between long-axis and inflow (angle 1 – angle 2), at the annulus level in this example. D: The positioning of the two reformat planes are shown at the annulus level and at the PIV-level, angulated perpendicular to the inflow. Left ventricle (LV), right ventricle (RV), left atrium (LA), and right atrium (RA).

the angle between long-axis and inflow at both levels (angle 1 – angle 2 and angle 1 – angle 3) (Fig. 1C). For these calculations, a positive value designates lateral inflow relative to the longaxis on the four-chamber view and anterior inflow relative to the long-axis on the two-chamber view. Intra- and interobserver variation of these angle measurements was tested by repeated analysis in 10 randomly selected controls and 10 patients. Two observers (E.C. with 2 years of cardiac MRI experience and J.W. with over 15 years of cardiac MRI experience) performed these analyses blinded for each other, with one observer (E.C.) performing the analyses twice with an interexamination time of 3 weeks.

Image Analysis: Quantification of LAVV Forward Flow

LAVV velocity mapping was performed retrospectively. For comparison with the clinically used 2D technique, a static fixed MPR was defined retrospectively as described previously on the annulus at the moment of end systole by an MRI technician (P.v.d.B.) with over 20 years of experience. For 4DFlow quantification, two MPR measurement planes were positioned retrospectively: one on the anatomical annulus and one at the level of PIV distal to the annulus and angulated perpendicular to the inflow direction, using streamline visualization (Fig. 1D). The 4DFlow quantification analysis was performed by one observer (E.C.) with 2 years of experience in cardiac MRI and verified by one experienced observer with more than 15 years of experience in cardiac MRI (J.W.). Solely during systole, the reformat plane was positioned as previously described, either at the closed valve or, in case of regurgitation, 1–1.5 cm proximal to the valve inside the atrium, perpendicular to the jet [12]. Transvalvular flow velocity was calculated by subtraction of myocardial velocity in the throughplane direction, sampled in nearby myocardium, from the mean inflow velocity. Transvalvular flow volume was subsequently calculated by integrating the transvalvular velocity over the inflow area (ie, the flow rate) and then integrating over the cardiac cycle. Because we aimed to evaluate quantification approaches of left ventricular inflow only, the same regurgitation volume during systole as most optimally quantified was included in all three measurements. Finally, the flow volume at the aortic valve was assessed from the same 4DFlow MRI data aligned on a coronal and sagittal aorta view [12], to evaluate correlation and agreement with trans-LAVV effective forward flow.

Statistical Analysis

Data analysis was performed using SPSS Statistics (v. 20.0 IBM SPSS, Chicago, IL) software. Variables were tested for normal distribution using the Shapiro–Wilk test. Continuous variables are expressed as mean ± standard deviation or median with interquartile range (IQR) where appropriate. Differences between patients and controls were determined using an unpaired T-test or Mann-Whitney-U-test. Differences in angles at E- and A-peak were tested with paired T-tests or Wilcoxon-Signed-Rank-test. Linear regression analysis and Bland-Altman analysis [13] were used to assess relation and agreement between LAVV effective forward flow and aortic flow. Intra- and interobserver variation was determined by the significance of differences between measurements and the intraclass correlation coefficient for absolute agreement and the coefficients of variance. A p-value<0.05 was considered as statistically significant. For statistical nonsignificant results (P > 0.05), the mean difference and 95% confidence interval (CI) of the difference are given.

RESULTS

Subject Characterization

Of 28 scanned patients, two were excluded because they had a restrictive LAVV ring placed around the annulus, made of paramagnetic material, which resulted in distortion of the MRI signal. One other patient was diagnosed with left isomerism and was excluded to avoid influence on inflow direction, due to atrial isomerism and different position of the heart. 4DFlow scans of the remaining 25 patients and 25 controls were visually inspected to be free from imaging artifacts and approved to be of adequate quality for image analysis. In all these patients and controls streamline visualization and trans-valvular flow quantification was possible. Patient and control characteristics are given in Table 1. Fifteen (60%) patients underwent correction of a partial AVSD and 10 (40%) of a complete AVSD. Correction of the AVSD involved closure of the cleft of the LAVV in 21 (84%) patients. Ejection fraction was significantly lower in patients compared with controls (55% (IQR 53–58) versus 61% (IQR 58–66), P < 0.001) and regurgitation volume was higher in patients compared with controls (8 mL (IQR 5–12) versus 1 mL (IQR 0–2), P < 0.001).

Table 1. Patient characteristics: Data are presented as mean ± standard deviation or median with interquartile range where appropriate. * indicates p<0.001. BSA = Body surface area, LVED = Left ventricular end diastolic volume, EF = Ejection fraction, AVSD = Atrioventricular septal defect, LAVV = Left atrioventricular valve.

	Controls (N=25)	Patients (N=25)
Age (yrs)	17 (IQR 12–28)	22 (IQR 16–31)
Male (N, %)	10 (40)	7 (28)
BSA (m^2)	1.6 ± 0.3	1.7 ± 0.4
LVED/BSA (mL/m^2)	87 ± 11	89 ± 16
EF (%)	61 (IQR 58–66)	55 (IQR 53–58)*
Regurgitation volume LAVV (mL)	1 (IQR 0–2)	8 (IQR 5–12)*
Time after surgical correction of AVSD (years)		19 ± 8

Healthy Controls

The angle measurements are presented in Table 2. On the four-chamber view, the inflow angle was larger during A-peak, implicating a more lateral inflow direction (E-peak 12±9° versus A-peak 17±7°, p=0.021). The difference in inflow angle between A- and E-peak ranged between −13 and 22. The difference between A- relative to E-peak correlated with age (R 0.573, P = 0.003).

Table 2. Inflow angles: angle measurements in the four-chamber view and two-chamber view in degrees at early (E) and late (A) filling. * (p < 0.05) and ** (p < 0.01) indicating statistical significant differences between patients and controls. Data are presented as mean ± standard deviation or median with interquartile range where appropriate.

		Four-chamber		Two-chamber	
		Controls	Patients	Controls	Patients
E	Annulus - long axis (angle 1)	95 ±3	98 ± 9	94 ± 6	101 ± 8**
	Annulus - inflow at annulus (angle 2)	83 ±9	88 ± 8	89 ± 10	94 ± 8*
	Inflow angle at annulus level (angle 1-2)	12 ± 9	10 ± 10	6 ± 9	7 ± 9
	Distance between annulus and PIV-level (mm)	14 ± 6	15 ± 6	13 ± 5	16 ± 6
	Annulus - inflow at PIV-level (angle 3)	84 (80–90)	77 (65–82)**	90 ± 7	92 ± 8
	Inflow angle at PIV-level (angle 1-3)	10 ± 8	19 ± 11**	5 ± 7	9 ± 9
A	Annulus - long axis (angle 1)	94 ± 4	102 ± 8**	98 ± 5	101 ± 8
	Annulus - inflow at annulus (angle 2)	77 ± 8	85 ± 12**	89 ± 10	100 ± 8**
	Inflow angle at annulus level (angle 1-2)	17 ± 7	16 ± 15	9 ± 10	2 ± 11*

On the two-chamber view, the inflow was more anterior relative to the long-axis at the A-peak (E-peak 6±9° versus A-peak 9±10°, p=0.034), with an intersubject range in difference from –14 to 13. The difference between inflow angle at PIV-level and annulus level was not statistically significant (mean difference 1.8 with 95% CI –0.6-4.5°, P =0.145). Velocities and flow volumes are provided in Table 3. In controls, high correlation was found between aortic flow volume and LAVV effective forward flow volume assessed with the 4DFlow MPR tracking the annular level (R^2 0.949, P < 0.001) and the 4DFlow MPR tracking the PIV-level and angulated perpendicular to inflow (R^2 0.949, P < 0.001), while correlation with static 2D MPR was lower (R^2 0.877, P < 0.001). The absolute error with aortic flow in volunteers was smaller when 4D MPR tracking the annulus (3 (1–8) mL, P = 0.001) and tracking PIV-level angulated on the inflow (3 (2–5) mL, P < 0.001) were used compared with the measurements with static 2D MPR (7 (4–16) mL). The mean difference between aortic flow volume and LAVV flow volume with 4D MPR tracking the annulus was 0.14 6 6.4 mL; 95% limit of agreement –12.4-12.7 mL and with 4D MPR tracking the PIVlevel and angulated on the inflow was –0.8 ± 4.6 mL; 95% limit of agreement –9.7-8.1 mL. The mean difference between aorta flow volume an LAVV flow from the static 2D MPR was higher with a mean difference of –10.1 ± 10.2 mL; 95% limit of agreement –30.0-9.9 mL (Fig. 2).

Patients

The inflow angle measurements performed in the patients are presented in Table 2. On the four-chamber view, the difference in inflow angle between E-peak and A-peak at annulus level was not statistically significant (mean difference 3.5° 95% CI –12.9– 1.5°, P = 0.113); however, a large interpatient variation was observed (range –40° to 38°). On the two-chamber view, inflow direction relative to the longaxis was more posterior during the A-peak (E-peak 7±9° versus A-peak 2±11°, p=0.009). In patients, the inflow direction at the PIV-level was more lateral compared with the inflow angle at annulus level (annulus 10±10° versus PIV-level 19±11°, p=0.003). In the

Table 3. Comparison of velocities and flow volumes: differences between trans- left atrioventricular valve (LAVV) velocity mapping using the static 2D MPR during diastole and a 4D MPR tracking the annulus and tracking the Peak inflow velocity (PIV)-level and angulated perpendicular to the inflow direction. Data are presented as mean ± standard deviation or median with interquartile range where appropriate, with * (p < 0.01) and ** (p < 0.001) indicating statistical significance between measurements with static 2D MPR and on the 4D MPR tracking the annulus level compared with the measurements with 4D MPR tracking the PIV-level and angulated perpendicular to the inflow direction. LAVV= left atrioventricular valve, PIV = Peak inflow velocity.

	Controls			Patients		
Reformat plane	Static 2D	4D annulus	4D PIV and angulated	Static 2D	4D annulus	4D PIV and angulated
LAVV flow volume (mL)	87 ± 26**	77 ± 20	78 ± 20	72 ± 21	65 ± 19**	70 ± 20
Absolute error LAVV flow with aortic flow (mL)	7 (4–16) **	3 (1–8)	3 (2–5)	4 (1–9) *	6 (2–10) *	2 (1–4)
Correlation LAVV flow with aortic flow (R^2)	0.877	0.950	0.949	0.823	0.877	0.972
Aortic flow (mL)		77 ± 20			71 ± 20	

3.2

two-chamber view, the difference in inflow angle between the two planes was not statistically significant (mean difference –2.3°, 95% CI –5.1–0.4°, P = 0.091). Flow volumes and velocities obtained at the two measurement positions are presented in Table 3. In patients, a higher correlation was found between aortic flow and LAVV flow measurements performed at the PIV-level with 4D MPR angulated perpendicular to inflow direction (R^2 0.972, P < 0.001) and with 4D MPR tracking the annulus (R^2 0.877, P < 0.001) rather than with the static 2D MPR (R^2 0.823, P < 0.001). The absolute error between LAVV forward flow and aorta flow was smaller in the angulated MPR at the PIV–level (2 (1–4) mL), compared with MPR tracking the annulus (6 (2–10) mL, P = 0.003) and the static 2D MPR (4 (1–9) mL, P = 0.004). The mean difference between aortic flow and LAVV flow was smaller when the angulated MPR on PIV-level was used (0.2±3.4 mL; 95%-limit of agreement -6.9-6.4mL), compared with the MPR tracking the annulus (4.4 ±7.2mL; 95%-limit of agreement -9.6-18.5mL) and the static 2D MPR (-3.0±9.0 mL; 95%-limit of agreement -20.7-14.77mL).

Differences Between Patients and Healthy Controls

Differences in angle measurements between patients and healthy controls are given in Table 2. At the annulus level, the difference in inflow direction between patients and controls was not statistically significant (mean difference 2.0°, 95% CI –3.6-7.5°, P = 0.483). However, at the PIV-level, inflow direction was significantly more lateral (controls 10 ± 8° versus patients 19 ± 11°, P = 0.002) (Fig. 3). On the two-chamber view, the difference in inflow angle was not statistically significant between patients and controls during E-peak at both measurement levels (annulus mean difference 1.1°, 95% CI –6.1–3.9°, P = 0.668 and the PIV-level mean difference –4.1°, 95% CI –8.6–0.4°, P = 0.072), but the inflow was more posterior in the patients during Apeak (controls 9 ± 10° versus patients 2 ± 11°, P = 0.019).

Table 4. inter-observer and intra-observer analysis of angle measurements performed in the four- chamber view (4ch) and two-chamber view (2ch) during early (E) and late (A) filling. chamber view (4ch) and two-chamber view (2ch) during early (E) and late (A) filling. Ch = chamber.

	Inter-observer					Intra-observer				
	Intraclass correlation coefficient	Mean difference	p value	95% - Confidence interval	Coefficient of variation	Intraclass correlation coefficient	Mean difference	p value	95% - Confidence interval	Coefficient of variation
4ch angle 1 E peak	0.95 (p<0.001)	-0.1	0.932	-1.3, 1.2	3%	0.87 (p<0.001)	-1.5	0.069	-3.2, 0.1	4%
4ch angle 2 E peak	0.94 (p<0.001)	-0.3	0.685	-1.8, 1.2	4%	0.94 (p<0.001)	-1.3	0.069	-2.7, 0.1	4%
4ch angle 3 E peak	0.90 (p<0.001)	-1.9	0.127	-4.4, 0.6	7%	0.95 (p<0.001)	-1.5	0.096	-3.4, 0.3	5%
4ch angle 1 A peak	0.84 (p<0.001)	0.6	0.480	-1.2, 2.4	4%	0.89 (p<0.001)	0.15	0.830	-1.4, 1.7	3%
4ch angle 2 A peak	0.86 (p<0.001)	0.1	0.965	-2.4, 2.5	8%	0.90 (p<0.001)	0.0	1.000	2.1, 2.1	5%
2ch angle 1 E peak	0.92 (p<0.001)	-1.4	0.072	-2.9, 0.2	3%	0.77 (p<0.001)	-1.5	0.199	-3.9, 0.9	5%
2ch angle 2 E peak	0.93 (p<0.001)	0.2	0.811	-1.5, 1.9	4%	0.88 (p<0.001)	-0.3	0.783	-2.5, 2.0	6%
2ch angle 3 E peak	0.92 (p<0.001)	-1.2	0.192	-2.9, 0.6	4%	0.82 (p<0.001)	-0.3	0.798	-2.7, 2.1	7%
2ch angle 1 A peak	0.93 (p<0.001)	-1.9	0.005	-3.1, -0.6	3%	0.89 (p<0.001)	-0.6	0.453	-2.2, 1.0	3%
2ch angle 2 A peak	0.97 (p<0.001)	-1.3	0.129	-2.9, 0.4	4%	0.93 (p<0.001)	0.0	1.000	-2.1, 2.1	4%

Inter- and Intraobserver Variation

Interobserver coefficient of variation for angle measurements ranged between 3% and 8%, with an intra-class correlation coefficient higher or equal to 0.85 ($P < 0.001$). The mean differences ranged between 0.1° and 1.9° and none of these were statistically significant, except for the assessment of the angle between two-chamber view annulus and long-axis (mean difference 1.9 ± 2.7°, $P = 0.005$). The intraobserver coeffi- cient of variation ranged between 3% and 7%, with an intraclass correlation coefficient higher or equal to 0.77 ($P < 0.001$) and differences ranged between 0° and 1.5° (Table 4).

Figure 2. Agreement between left atrioventricular valve (LAVV) forward flow and aorta flow using three approaches for MPR placement.

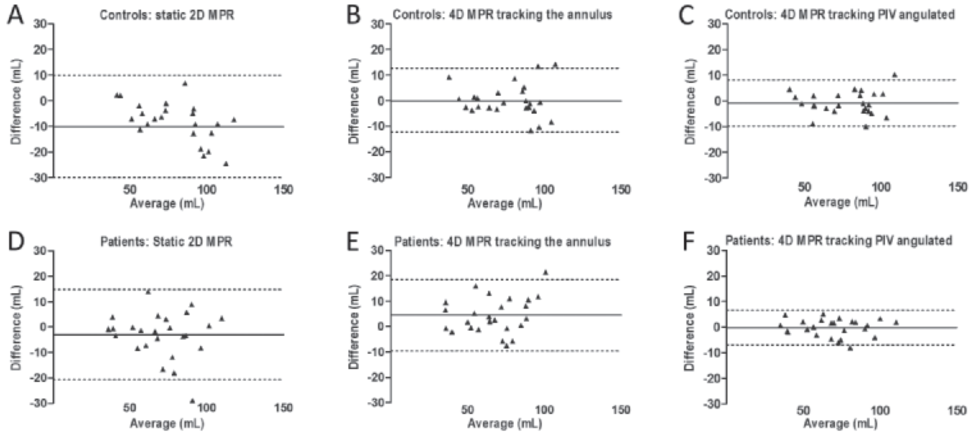

Bland–Altman graphs depicting agreement between aortic flow and effective forward flow over the LAVV with static 2D MPR (A,D), 4D MPR tracking the annulus (B,E) and 4D MPR tracking peak inflow velocity (PIV)-level and angulated perpendicular to the inflow (C,F), measured both in controls (A–C) as well as in corrected atrioventricular septal defect (AVSD) patients (D–F).

DISCUSSION

In this study, streamline visualization of 4DFlow MRI data was used to characterize and improve the quantification of trans-LAVV forward flow in healthy controls and patients after AVSD correction. The main findings of the current study are as follows: First, streamline visualization revealed a change in inflow direction between E- and A-peak in healthy controls and patients and a more laterally directed LV inflow in patients with corrected AVSD. Second, streamline visualization aids in optimizing the positioning and angulation of the measurement plane (ie, at peak inflow velocity level and perpendicular to inflow direction) during retrospective valve tracking procedure, resulting in a more reliable assessment of trans-LAVV forward flow volume in patients.

Quantification and characterization of transatrioventricular valve flow is important in the evaluation of ventricular and valvular function. In the healthy subjects, we observed a difference in

Figure 3. Lateral inflow after AVSD correction.

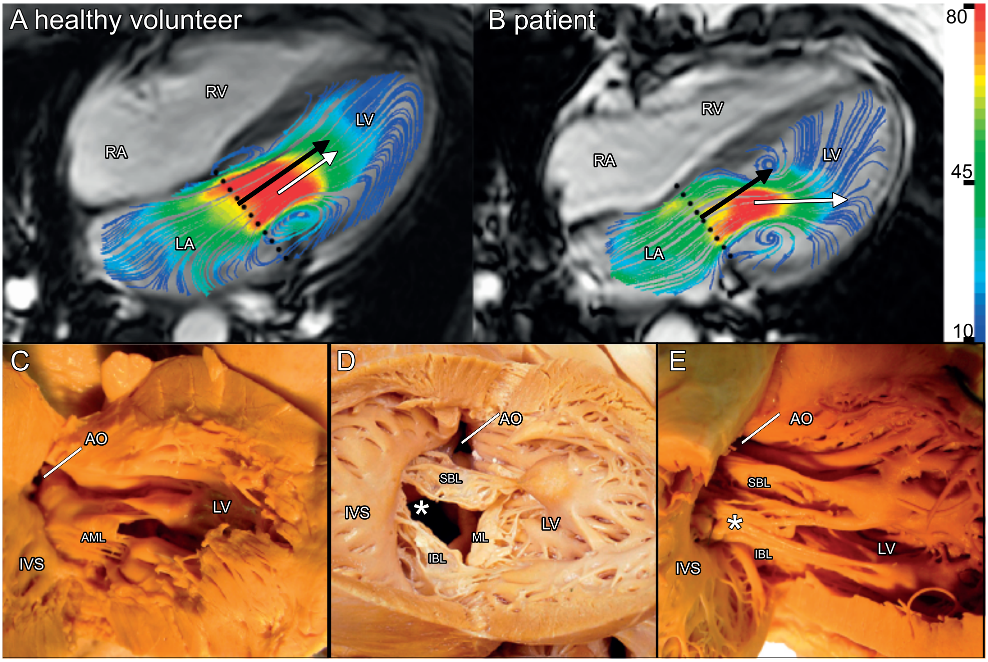

Streamline representation with velocity color coding (in cm/s) of the LV inflow pattern, illustrating the difference in inflow direction at E-peak inflow between a healthy volunteer (A) and a corrected AVSD patient (B), which presents with a more lateral inflow. The dotted line represents the annulus. Black arrow points in the direction of the inflow at the annulus level and the white arrow depicts the inflow direction at the peak inflow velocity (PIV)-level. C: A normal mitral valve with supple anterior leaflet of the mitral valve (AML). D: An AVSD before surgery with the ridged superior bridging leaflet (SBL), inferior bridging leaflet (IBL), and mural leaflet (ML); *the cleft. E: An AVSD heart after correction; the cleft between the SBL and IBL was closed (*). Left ventricle (LV), right ventricle (RV), left atrium (LA) and right atrium (RA), aorta (AO), interventricular septum (IVS).

inflow angle at E- and A-peak in both the four-chamber as well as the two-chamber orientation, which is most likely explained by the incomplete opening of the LAVV during A-peak phase [14]. Our observations are in line with Fyrenius et al [10] and extend their observations by quantification of the inflow angle. The high degree of intersubject variability correlated with age, where in younger patients the A-peak inflow was relatively more lateral compared with the E-peak. To investigate this further, a larger number of subjects and a broader age range is required. The intersubject variation in inflow angle, the difference between inflow angle at E- versus A-peak in both four- and two-chamber view implies that adjustment of the reformatting plane with 4DFlow MRI in each patient and during the whole cardiac cycle is relevant for quantification and characterization of trans-atrioventricular valve flow.

The observed dynamic changes in inflow direction during E- versus A-peak in healthy subjects were statistically significant but small, with substantial intersubject variation. The clinical relevance of these findings needs to be investigated in future studies. The PIV-level was found on average 15–16 mm distal to the annulus, corresponding with approximately half of the diameter of the LAVV, suggesting that the measured peak velocity may be found near or at the tip of the LAVV leaflets. At this PIV-level, the inflow direction in patients was directed significantly more laterally. The altered inflow is presumably caused by the abnormal annulus shape and attachment of the anterolateral papillary muscle as described in a previous echocardiography study in corrected AVSD patients [4] and by the restrictive mobility of the septal leaflet caused by the cleft closure during correction (Fig. 3). Future studies are needed to investigate whether regurgitation of the LAVV effects the inflow direction.

Lateral inflow was previously found in patients with dilated LVs [15] and the altered flow pattern in patients with dilated cardiomyopathy was related to an increased loss in kinetic energy [16]. In simulations with computational fluid dynamics, changes in eccentricity of the inflow jet have been shown to reduce the efficiency of the heart pump by 10% [3]. Further studies are required to investigate whether the aberrant inflow pattern after correction of AVSD, indeed, in addition to other factors, contributes to less efficient LV function. These insights may be valuable in changing surgical techniques to minimize leaflet restriction and, subsequently, the effect on LV function. The more lateral inflow direction in patients with a corrected AVSD should also be taken into account during Doppler echocardiography. Appleton et al [14] observed that in patients with a dilated LV, the inflow can be directed up to 20 more lateral, leading to changes in inflow velocity recording without proper alignment of the echo Doppler beam to peak velocity direction and level. This report and our observation of a more lateral inflow in patients after AVSD correction stresses the need for proper adjustment to the inflow direction using echocardiography. The higher flow volume measured in controls, using the static 2D MPR approach, confirms previously described overestimation of LAVV when a static plane is used, due to movement of the atrioventricular valve [17]. The overestimation of flow was not observed in the patients, which can be explained by reduced throughplane movement of the AV valve but, more important, a concomitant increased misalignment due to the observed angulated flow, which compensates the overestimation.

Furthermore, in patients we found a higher accuracy in trans-LAVV flow quantification when measurements were performed at the PIV-level angulated to the inflow, with an underestimation of flow when the measurement plane was tracking the annulus. This is possibly caused by the difficulty in defining the exact anatomical position and angulation of the annulus in patients with corrected AVSD and the increased deviation of the inflow angle in these patients. Furthermore, while the effect of intravoxel phase dispersion and partial volume on the measured vector components contributing to the velocity mapping procedure will not change when the reformatting plane is adjusted in a 4DFlow dataset, higher accuracy can still be achieved by reducing the number of voxels with such inaccurate velocity within the region of interest due to a better alignment of the measurement plane perpendicular to the flow [9]. The higher accuracy stresses the importance of streamline visualization in 4DFlow quantification to optimize positioning of the measurement plane. Further studies are required to investigate the impact of optimal positioning of the measurement plane in other congenital and acquired heart disease.

Our study has some limitations. Streamline visualization of 4DFlow MRI data is projected onto two- and four-chamber views and subsequently used for manual angle measurements and adjustment of measurement planes and, therefore, anatomical information and streamline data originate from different scans. Streamlines are a representation of the instantaneous flow velocity field and do not visualize the actual timecontinuous pathway of blood particles as pathlines do. In the present study we aimed to use the streamline visualization of the inflow direction at each specific timepoint during diastole and use this to position the measurement plane (assessing flow volume as through-plane velocity times cross-sectional area) at each of these timepoints. However, future studies may focus on differences between streamline and pathline visualization and their effect on measurement plane positioning. Differences in heart rate and respiratory rate might have caused some inaccuracy. In the future, automatic positioning and adjustment of measurement planes to the inflow direction from single scan data might improve the reliability and reproducibility of inflow assessment. All scans were performed with free-breathing and 4DFlow acquisition was performed without navigator gating in order to minimize acquisition time, because children were included in the study. However, image quality was adequate in all studies to perform offline velocity mapping and any possible effect of overestimation in flow volume due to area enlargement from breathing motion may be assumed to be equal in patients and controls. Local phase offset errors, which may lead to small systematic errors, should be taken into account [18]. During data reconstruction, the commercially available concomitant gradient correction and local phase correction filter were applied. Furthermore, measurements of peak velocity at the annulus level and at the PIVlevel were obtained from the same dataset at sampling positions relatively close to each other and, therefore, we may assume that a potential systematic error in velocity is almost equal for both sampling positions. Furthermore, for LAVV flow quantification, transvalvular velocity is calculated from local blood flow velocity relative to through-plane myocardial velocity and is therefore corrected for potential phase offset errors.

CONCLUSION

Streamline visualization of 4DFlow MRI data confirmed different inflow angle at early versus late filling in healthy controls, with substantial intersubject variation and a more laterally orientated LV inflow after AVSD correction. Using this visualization for optimizing the position of the measurement plane, assessment of trans-LAVV blood flow proved to be more accurate and resulted in related changes in blood flow characteristics. Our findings have implications for the assessment of trans-LAVV flow, as they stress the importance of careful adjustment of echocardiography Doppler beam or MRI measurement plane in the assessment of the dynamic ventricular inflow and taking into account alterations caused by AVSD correction.

REFERENCES

1. Bella JN, Palmieri V, Roman MJ, et al. Mitral ratio of peak early to late diastolic filling velocity as a predictor of mortality in middle-aged and elderly adults: the Strong Heart Study. Circulation 2002;105:1928–1933.
2. Little WC, Oh JK. Echocardiographic evaluation of diastolic function can be used to guide clinical care. Circulation 2009;120:802–809.
3. Pedrizzetti G, Domenichini F. Nature optimizes the swirling flow in the human left ventricle. Phys Rev Lett 2005;95:108101.
4. Takahashi K, Mackie AS, Thompson R, et al. Quantitative realtime three-dimensional echocardiography provides new insight into the mechanisms of mitral valve regurgitation post-repair of atrioventricular septal defect. J Am Soc Echocardiogr 2012;25: 1231–1244.
5. Napel S, Lee DH, Frayne R, Rutt BK. Visualizing threedimensional flow with simulated streamlines and threedimensional phase-contrast MR imaging. J Magn Reson Imaging 1992;2:143–153.
6. Nordmeyer S, Riesenkampff E, Messroghli D, et al. Four-dimensional velocity-encoded magnetic resonance imaging improves 8 Calkoen et al.blood flow quantification in patients with complex accelerated flow. J Magn Reson Imaging 2013;37:208–216.
7. Westenberg JJ, Danilouchkine MG, Doornbos J, et al. Accurate and reproducible mitral valvular blood flow measurement with three-directional velocity-encoded magnetic resonance imaging. J Cardiovasc Magn Reson 2004;6:767–776.
8. Westenberg JJ, Roes SD, Ajmone MN, et al. Mitral valve and tricuspid valve blood flow: accurate quantification with 3D velocityencoded MR imaging with retrospective valve tracking. Radiology 2008;249:792–800.
9. Lotz J, Meier C, Leppert A, et al. Cardiovascular flow measurement with phase-contrast MR imaging: basic facts and implementation. Radiographics 2002;22:651–671.
10. Fyrenius A, Wigstrom L, Bolger AF, et al. Pitfalls in Doppler evaluation of diastolic function: insight from 3-dimensional magnetic resonance imaging. J Am Soc Echocardiogr 1999;12:817–826.
11. Hoohenkerk GJ, Bruggemans EF, Rijlaarsdam M, et al. More than 30 years' experience with surgical correction of atrioventricular septal defects. Ann Thorac Surg 2010;90:1554–1561.
12. Roes SD, Hammer S, van der Geest RJ, et al. Flow assessment through four heart valves simultaneously using 3-dimensional 3- directional velocity-encoded magnetic resonance imaging with retrospective valve tracking in healthy volunteers and patients with valvular regurgitation. Invest Radiol 2009;44:669–675.
13. Bland JM, Altman DG. Statistical methods for assessing agreement between two methods of clinical measurement. Lancet 1986;1:307–310.
14. Appleton CP, Jensen JL, Hatle LK, et al. Doppler evaluation of left and right ventricular diastolic function: a technical guide for obtaining optimal flow velocity recordings. J Am Soc Echocardiogr 1997;10:271–292.
15. Mohiaddin RH. Flow patterns in the dilated ischemic left ventricle studied by MR imaging with velocity vector mapping. J Magn Reson Imaging 1995;5:493–498.
16. Eriksson J, Bolger AF, Ebbers T, et al. Four-dimensional blood flow-specific markers of LV dysfunction in dilated cardiomyopathy. Eur Heart J Cardiovasc Imaging 2013;14:417–424.
17. Kilner PJ, Gatehouse PD, Firmin DN. Flow measurement by magnetic resonance: a unique asset worth optimising. J Cardiovasc Magn Reson 2007;9:723–728.
18. Gatehouse PD, Rolf MP, Graves MJ, et al. Flow measurement by cardiovascular magnetic resonance: a multi-centre multi-vendor study of background phase offset errors that can compromise the accuracy of derived regurgitant or shunt flow measurements. J Cardiovasc Magn Reson 2010;12:5.